

Fracture assessment of polyacrylonitrile nanofiber-reinforced epoxy adhesive

S.M.J. Razavi¹, R. Esmaeely Neisiany^{2,3}, M.R. Ayatollahi⁴, S. Ramakrishna³, S. Nouri Khorasani², F. Berto¹

¹ *Department of Mechanical and Industrial Engineering, Norwegian University of Science and Technology (NTNU), Richard Birkelands vei 2b, 7491, Trondheim, Norway.*

² *Department of Chemical Engineering, Isfahan University of Technology, Isfahan 84156-83111, Iran.*

³ *Center for Nanofibers and Nanotechnology, Department of Mechanical Engineering, National University of Singapore (NUS), Singapore 117576, Singapore.*

⁴ *Fatigue and Fracture Lab., Centre of Excellence in Experimental Solid Mechanics and Dynamics, School of Mechanical Engineering, Iran University of Science and Technology, Narmak, 16846, Tehran, Iran.*

Abstract:

Electrospun polyacrylonitrile (PAN) nanofibers were incorporated in an epoxy-based adhesive layer to improve the adhesive joint's mechanical performance. The morphological study of the electrospun PAN nanofibers revealed that the fabricated nanofibers were smooth, continuous, and without beads. The average diameter of the nanofibers was determined to be 362 ± 87 nm. The Double Cantilever Beam (DCB) specimens were tested and the fracture energies were determined for the unreinforced and reinforced adhesives. The outstanding reinforcing capability of PAN nanofibers was demonstrated by significant improvements in fracture energy of the adhesive containing PAN nanofibers. A maximum improvement of 127% in the mode I fracture energy of adhesive was achieved by incorporating 2 g/m^2 of PAN nanofibers into the adhesive layer. Moreover, the morphology of the fracture surfaces was examined using the Scanning Electron Microscopy (SEM) technique to evaluate the toughening mechanisms resulting from this improvement.

Keywords: Adhesive joints; Electrospun polyacrylonitrile nanofibers; Energy release rate; Fracture energy.

1. Introduction

Adhesively bonding techniques provide substantial advantages over the traditional joining methods such as bolting, riveting and welding. Excellent resistance to mechanical loading beside lower weight has made the adhesive bonding an ideal joining technique in different industries. The epoxy-based adhesives have been considered as the most commonly used adhesives due to their favorite mechanical properties such as high modulus and strength. However, these types of adhesives usually suffer from low fracture toughness. In order to improve the mechanical behavior of adhesive joints, researchers have proposed several methods such as modifying the adhesive joint geometry [1,3] and adhesive layer reinforcement by adding nano, micro and macro additives [4-19]. Considering the nano-scale modification, several non-additives of various shapes and materials including single-walled carbon nano-tube [4], multi-walled carbon nano-tube [5,6], graphene and graphene oxide nano-platelet [7,8], nano-silica [9,10], silicon carbide whisker [11,12], nano-rubber [13,14] and nano-clay [15] have been widely investigated in order to improve mechanical properties of the adhesives.

Incorporating electrospun polymeric nanofibers as an interlaminar reinforcement in fiber reinforced polymers was studied in some recently published papers [20-23]. Advantages of incorporating the electrospun polymeric nanofibers as an interlaminar reinforcement in fiber reinforced polymeric composites have been reported in several previous researches [20-23]. Molnar et al., used PAN nanofibers, fabricated from

needleless electrospinning method, in order to reinforce mechanical properties of a conventional carbon/epoxy composite. They reported that PAN nanofibers were chosen due to their ductility and good adhesion to epoxy resin as matrix [20,21]. Neisiany et al., showed neither the epoxy resin nor its curing agent lead to any effects on PAN nanofibers or dissolve them [24]. They also showed that incorporation of both neat [22] and core-shell [23] PAN electrospun nanofibers between carbon layers leads to improvement in in-plane properties of carbon epoxy composite as well as its out-of-plane properties. The nano-fiber breakage and nanofiber pull out were reported as mechanisms for enhancing in-plane properties of the hybrid composites [20,21]. On the other hand, nanofibers act as means of stress transfer from the resin-rich area to the reinforcing phase (carbon fibers), and hence more uniform stress distribution of applied load in the resin-rich area occurs which leads to the enhancement in the composite out-of-plane properties [20,21].

The polymeric nanofibers, fabricated from facile and economical electrospinning method, can be also incorporated in the adhesive layer with various diameters and thicknesses of the reinforcing layer. In the present research, different amounts of the PAN nanofibers were added in an epoxy-based adhesive. DCB specimens, fabricated with the unreinforced and reinforced adhesives, were tested to evaluate the effect of nanofibers on the fracture behavior of the adhesive.

2. Experiments

2.1. Materials

The solvent-free two-component epoxy-based adhesive (UHU® plus endfest 300 adhesive) [25] was employed for experiments. Table 1 summarizes the specification of

UHU® plus endfest 300 adhesive. In order to prevent plastic deformation of the substrates, 7075-T651 aluminum was employed for fabricating the substrates due to high yield strength reported for this type of aluminum alloy (500 MPa). Standard uniaxial tensile tests [26,27] were conducted on substrates and adhesive to obtain their mechanical behavior as summarized in Table 2. In order to fabricate PAN nanofibers, PAN ($M_w = 150$ kDa) was purchased from Sigma-Aldrich, whereas N,N-Dimethylformamide (DMF, 99.8%) was supplied from Daejung chemical & metal Co.,Ltd and used as solvent of PAN.

2.2. Specimens Preparation

The geometry of DCB specimens is shown in Fig. 1. The 10 mm thick aluminum plates were used for fabrication of the substrates. The surface of aluminum plates was polished using 200-grit sandpaper to increase the roughness of surface and eventually improve the mechanical locking between the adhesive and aluminum. Afterward, the substrates were pre-treated using an acid etch according to DIN 53281 in order to enhance the adhesion between the adhesive and the substrates [28]. Table 3 presents the composition of the etching solution.

Prior to adding the PAN nanofibers in the adhesive layer, a thin layer of adhesive was supplied on both substrates. After that, the electrospinning method was used to incorporate the PAN nanofibers on bonding surface of one of the substrates. To avoid any damage to the PAN nanofibers, during the nanofiber fabrication and incorporation in the adhesive layer, the electrospun PAN nanofibers were directly deposited on the applied adhesive on the surfaces of aluminum substrate. The 10 wt% solution of PAN powder was combined with a proper amount of DMF solvent in a scintillation vial,

and stirred by a magnetic stirrer for 24 h at room temperature. The 10 wt% PAN solution was supplied to a syringe with needle gage 23. In order to have a stable electrospinning process for deposition of the PAN nanofibers on the bonding surface, the electrospinning parameters were adjusted as follows: The constant flow rate of 1 ml.h^{-1} was used for the PAN solution, while the distance between the needle tip and the collector (i.e. bond surface) was fixed at 15 cm, and a 16 kV direct current voltage was applied to induce the formation of nanofibres from the PAN solution. Fig. 2 illustrates diameter distribution curve for the electrospun PAN nanofiber.

As the key parameter in the experiments, average values of 1, 2 and 3 gr/m^2 PAN nanofibers were added to the adhesive layer. Then, 12 μm thick non-stick polyethylene film was placed in adhesive layer as the pre-crack. A pre-crack length of 20 mm was considered for all the test samples. The bond-line thickness was controlled using 0.15 mm thick spacers between the substrates. The test samples were placed inside the fabrication fixture to ensure the alignment of the substrates. The exploded view of adhesive joints made by nano-reinforced and reinforced adhesives is shown in Fig. 3. The test specimens were cured for one week at room temperature. For each specimen configuration, at least four samples were manufactured and tested.

2.3. Testing procedure

The DCB adhesive joints were tested under quasi-static loading with a constant displacement rate of 0.25 mm/min using an Instron ElectroPulsTM E10000 (Massachusetts-United States) universal testing machine with a 10 kN load cell to obtain the load-displacement ($P - \delta$) curves of the joints. All the fracture tests were conducted at temperature of approximately 20 °C and at 70% relative humidity. The crack propaga-

tion was tracked at 5 s intervals during testing using a digital camera (Canon EOS 600D with an EF 100 mm f/2.8 Macro Lens, Tokyo-Japan). Matte white color was sprayed on one side of DCB specimens to assist the crack tip observation. In addition, paper rulers were glued under the adhesive layer to enable the crack length (a) reading.

2.4. Fracture energy determination

The simple beam theory was used in this research to calculate the critical energy release rate (fracture energy) under pure mode I (G_{IC}) loadings. According to the simple beam theory, the fracture energy can be obtained by use of the applied load and crack length at each stage during testing. Considering the simple beam theory, the mode I fracture energy was calculated using Eq. (1) according to BS 7991 standard [29].

$$G_{IC} = \frac{4P^2}{Eb^2} \left(\frac{3a^2}{h^3} + \frac{1}{h} \right) \quad (1)$$

in which G_{IC} is the mode I fracture energy of the adhesive, P is the applied load, b is the width of substrates, h is the substrates thickness, a is the crack length, E is the elastic modulus of substrates.

3. Results and discussion

Fig. 4 illustrates typical experimental load-displacement curves related to the DCB specimens bonded by the non-reinforced and PAN reinforced adhesives. According to Fig. 4, incorporation of PAN nanofibers in the adhesive layer increased the load bear-

ing capacity of the DCB joints and consequently led to an enhancement of the fracture energy of the epoxy adhesive. Fig. 5 illustrates the representative R-curves (fracture energy versus crack length) of the tested adhesive joints, which were obtained using the simple beam theory.

Considering the variation of fracture energy by crack length, in order to compare the mode I fracture energies of the specimens with different reinforcements, fracture energy values were averaged over from crack length 30 mm up to 60 mm. In this case, the effect of pre-crack blunting and plasticity will be eliminated in the results. Table 4 presents the averaged fracture energies of the non-reinforced and PAN reinforced adhesives. According to Table 4, fracture energies of all reinforced adhesives were higher than that of the non-reinforced adhesive. The fracture energies of adhesives with PAN nanofibers continuously increased by increasing the amount of nano fibers from 1 g/m² to 2 g/m², however the fracture energy improvement for the adhesive reinforced by 3 g/m² PAN nanofiber showed a decrease compared with the reinforced adhesive containing 2 g/m². The experimental results revealed that for the reinforced adhesives with 1, 2 and 3 g/m² PAN nanofibers, the mode I fracture energies were improved about 45%, 127% and 55% compared to the non-reinforced adhesive. The PAN nanofibers act as bridge for transferring applied load from adhesive layer to aluminum substrate as well as stress distribution and reducing propagation of created crack in the adhesive layer [22,23]. It should be noted that, the observed reduction in the mode I fracture energy improvement of 3 g/m² PAN incorporation can be attributed to the enhancement in the nanofiber layer thickness. Increasing the nanofiber layer thickness leads to poor penetration of epoxy-based adhesive between nanofibers layer and subsequently decreasing the interaction between adhesive and the nanofibers.

Due to imperfect interaction between the epoxy adhesive (as matrix) and the nanofibers, the stress transfer from the adhesive to aluminum substrate could not completely occur and consequently the mechanical properties decreased [30,31].

In order to investigate the effect of PAN nanofibers on the failure mechanisms of the reinforced adhesive (with higher fracture energies), SEM with an acceleration voltage of 30.00 kV was used to examine the morphology of the fracture surfaces. The SEM micrographs of the fracture surfaces of the unreinforced and reinforced adhesives with different amounts of electrospun PAN nanofibers are shown in Fig. 6.

According to Figs. 6(b-d), the fracture surfaces of reinforced adhesives were quite rougher than that of the neat adhesive (Fig. 6a). This can be accounted as an important reason of the improvement in the fracture energy due to adding PAN nanofibers, as rougher fracture surfaces need higher energy to develop. When the adhesive joints are loaded, extension of micro-cracks may encounter PAN nanofibers; since, due to striking characteristics of PAN nanofibers, the micro-cracks are forced to either round the fibers or be pinned. In this situation, the micro-cracks require more externally applied load to propagate.

The PAN nanofibers were cold worked during the electrospinning process, resulting in its high strength and leading to a better stress distribution in the adhesive layer. Since the PAN nanofibers are stiffer than the matrix, when the matrix is subjected to elastic deformation, the PAN nanofibers delay the matrix deformation. This results in plastic deformation of matrix around the PAN nanofibers (because of stress concentration) and consumption of considerable amounts of energy.

As mentioned before, various nano/micro additives have been used by researchers to improve the mechanical behavior of the adhesive. Wernik et al. [32] incorporated

multi-walled carbon nano-tubes in an epoxy based adhesive and achieved 36% improvement in the mode I fracture energy. Khoramishad and Khakzad [33] improved an epoxy adhesive with multi-walled carbon nano-tubes. They reported a maximum improvement of 58.4% in the adhesive fracture energy when 0.3 wt% of multi-walled carbon nano-tubes were incorporated into the adhesive.

Comparing the experimental data presented in the current research with the experimental data available in the literature revealed that considerably higher fracture energy improvements were obtained for the PAN nano fiber reinforced epoxy adhesive.

4. Conclusions

Effect of PAN electrospun nanofibers on the fracture behavior of an epoxy adhesive was experimentally studied. Different amounts of PAN nanofibers were incorporated in the adhesive layer of DCB specimens. The specimens were then tested under pure mode I loading. A comparison between the neat and reinforced adhesives, indicated that the addition of PAN nanofibers increased the fracture energy of adhesive base from initial value of 0.11 N/mm to 0.25 N/mm for reinforced adhesive. The maximum obtained enhancement was equal to 127%. The PAN nanofibers showed a high potential in improving the fracture strength of the epoxy adhesives. Increased energy absorption of adhesive layer during failure of reinforced adhesives was further supported by observations from the SEM pictures of fracture surfaces of the tested joints.

References

- [1] S.M.J. Razavi, E. Esmaeili, M. Samari, S.M.R. Razavi, Stress analysis on a non-flat interface bonded joint, *J. Adhes.* (in Press) (DOI: 10.1080/00218464.2016.1257942)
- [2] M.R. Ayatollahi, M. Samari, S.M.J. Razavi, L.F.M. da Silva, Fatigue performance of adhesively bonded single lap joints with non-flat sinusoidal interfaces, *Fatigue Fract. Eng. Mater. Struct.* (in press) (DOI: 10.1111/ffe.12575)
- [3] S.M.J. Razavi, F. Berto, M. Peron, J. Torgersen, Parametric study of adhesive joints with non-flat sinusoid interfaces, *Theor. Appl. Fract. Mech.* (in press) (DOI: 10.1016/j.tafmec.2017.06.019)
- [4] A. Ahmed khan, A.A. Al Kheraif, J. Syed, D.D. Divakar, J.P. Matinlinna, Enhanced resin zirconia adhesion with carbon nanotubes infused silanes: A pilot study, *J. Adhes.* (in press).
- [5] M.R. Ayatollahi, A. Nemati Giv, S.M.J. Razavi, H. Khoramishad, Mechanical properties of adhesively single lap bonded joints reinforced with multi-walled carbon nanotubes and silica nanoparticles. *J. Adhes.* (in press) (DOI: 10.1080/00218464.2016.1187069)
- [6] W. Zielecki, A. Kubit, T. Trzepiecinski, U. Narkiewicz, Z. Czech, Impact of multiwall carbon nanotubes on the fatigue strength of adhesive joints. *Int. J. Adhes. Adhes.* 73 (2017) 16-21.
- [7] A. Kausar, Z. Anwar, B. Muhammad, An Overview of Non-Flammability Characteristics of Graphene and Graphene Oxide-Based Polymeric Composite and Essential Flame Retardancy Techniques, *J. Adhes.* (in press) (DOI: 10.1080/03602559.2016.1233274)

- [8] Q. Liu, Q. Xu, Q. Yu, R. Gao, T. Tong, Experimental investigation on mechanical and piezoresistive properties of cementitious materials containing graphene and graphene oxide nanoplatelets, *Constr. Build Mater.* 127 (2016) 565-576.
- [9] M.K. Jang, S.K. Lee, B.K. Kim, Polyurethane nano-composite with functionalized silica particle, *Compos. Interfaces* 15(6) (2008) 549-559.
- [10] H.A. Bahgat, E. Alshwaimi, A.E. El-Embaby, Evaluation of the bonding ability of a nano-structured adhesive system, *Int. J. Dent. Sci. Res.* 2(2-3) (2015) 34-40.
- [11] M. Wang, R. Miao, J. He, X. Xu, J. Liu, H. Du, Silicon Carbide whiskers reinforced polymer-based adhesive for joining C/C composites, *Mater. Design* 99 (2016) 293-302.
- [12] M. Naeimirad, A. Zadhoush, R.E. Neisiany, Fabrication and characterization of silicon carbide/epoxy nanocomposite using silicon carbide nanowhisker and nanoparticle reinforcements, *J. Compos. Mater.* 50 (2016) 435-446.
- [13] A.J. Kinloch, J.H. Lee, A.C. Taylor, S. Sprenger, C. Eger, D. Egan, Toughening structural adhesives via nano- and micro-phase inclusions, *J. Adhes.* 79(8-9) (2003) 867-873.
- [14] F. Zairi, M.N. Abdelaziz, K. Woznica, J.M. Gloaguen, Constitutive equations for the viscoplastic-damage behaviour of a rubber-modified polymer, *Eur. J. Mech. A-Solid* 24(1) (2005) 169-182.
- [15] B.C. Kim, S.W. Park, D.G. Lee, Fracture toughness of the nano-particle reinforced epoxy composite, *Compos. Struct.* 86(1-3) (2008) 69-77.
- [16] H. Khoramishad, S.M.J. Razavi, Metallic Fiber-Reinforced Adhesively Bonded Joints, *Int. J. Adhes. Adhes.* 55 (2014) 114-122.

- [17] E. Esmaeili, S.M.J. Razavi, M. Bayat, F. Berto, On the flexural behavior of metallic fiber reinforced adhesively bonded single lap joints, *J. Adhes.* (in press) (DOI: 10.1080/00218464.2017.1285235)
- [18] S.M.J. Razavi, M.R. Ayatollahi, E. Esmaeili, L.F.M. da Silva, Mixed mode fracture response of a metallic fiber-reinforced epoxy adhesive, *Eur. J. Mech. A-Solids* 65 (2017) 349–359. (DOI: 10.1016/j.euromechsol.2017.06.001)
- [19] A. Nemati Giv, M.R. Ayatollahi, S.M.J. Razavi, H. Khoramishad, The Effect of orientations of metal macrofiber reinforcements on the mechanical properties of adhesively bonded single lap joints, *J. Adhes.* (in press) (DOI: 10.1080/00218464.2017.1305270)
- [20] K. Molnar, E. Kostakova, L. Meszaros, The effect of needleless electrospun nanofibrous interleaves on mechanical properties of carbon fabrics/epoxy laminates, *Express Polym. Lett.* 8(1) (2014) 62–72.
- [21] S.V. Lomov, K. Molnar, Compressibility of carbon fabrics with needleless electrospun PAN nanofibrous interleaves, *Express Polym. Lett.* 10(1) (2016) 25–35.
- [22] R. Esmaeely Neisiany, S. Nouri Khorasani, M. Naeimirad, J. Kong Yoong Lee, S. Ramakrishna, Improving Mechanical Properties of Carbon/Epoxy Composite by Incorporating Functionalized Electrospun Polyacrylonitrile Nanofibers, *Macromol. Mater. Eng.* 302 (2017) 1600551.
- [23] R.E. Neisiany, J.K.Y. Lee, S.N. Khorasani, S. Ramakrishna, Self-healing and interfacially toughened carbon fibre-epoxy composites based on electrospun core-shell nanofibres, *J. Appl. Polym. Sci.* 134 (2017) 44956.

- [24] R.E. Neisiany, S.N. Khorasani, J. Kong Yoong Lee, S. Ramakrishna, Encapsulation of epoxy and amine curing agent in PAN nanofibers by coaxial electrospinning for self-healing purposes, *RSC Adv.* 6 (2016) 70056-70063.
- [25] UHU plus endfest 300 technical data sheet, https://media2.supermagnete.de/docs/uhu_plus_endfest_300_eng.pdf (accessed: 04.06.2017)
- [26] ASTM E8 / E8M-15a, Standard Test Methods for Tension Testing of Metallic Materials, ASTM International, West Conshohocken, PA, 2015.
- [27] ASTM D638-14, Standard Test Method for Tensile Properties of Plastics, ASTM International, West Conshohocken, PA, 2014.
- [28] German Institute for standardization (DIN). DIN 53281: Testing of adhesively bonded joints-Preparation of test specimens. Berlin: German standard; 2006.
- [29] BS 7991, Determination of the mode I adhesive fracture energy, GIC, of structural adhesives using the double cantilever beam (DCB) and tapered double cantilever beam (TDCB) specimens, British Standard, 2001.
- [30] R.E. Neisiany, J.K.Y. Lee, S.N. Khorasani, S. Ramakrishna, Towards the development of self-healing carbon/epoxy composites with improved potential provided by efficient encapsulation of healing agents in core-shell nanofibers, *Polymer Testing* 62 (2017) 79-87.
- [31] Q. Chen, Y. Zhao, Z. Zhou, A. Rahman, X.F. Wu, W. Wu, T. Xu, H. Fong, Fabrication and mechanical properties of hybrid multi-scale epoxy composites reinforced with conventional carbon fiber fabrics surface-attached with electrospun carbon nanofiber mats, *Compos. Part B: Eng.* 44(1) (2013) 1-7.

[32] J. Wernik, S. Meguid, On the mechanical characterization of carbon nanotube reinforced epoxy adhesives, *Mater. Design* 59 (2014) 19-32.

[33] H. Khoramishad, M. Khakzad, Toughening Epoxy Adhesives with Multi-Walled Carbon Nanotubes, *J. Adhes.* (in press). (DOI: 10.1080/00218464.2016.1224184)

Table captions:

Table 1. Specifications of adhesive UHU plus endfest 300 [25].

Table 2. The mechanical properties of the adherends and adhesive.

Table 3. Composition of etching solution for aluminum adherends [28].

Table 4. Fracture energies obtained from experiments.

Figure captions:

Fig. 1. Schematic geometry of the DCB test specimen (dimensions in mm).

Fig. 2. Diameter distribution curve of PAN nanofibers.

Fig. 3. Exploded view of adhesive joints bonded by (a) non-reinforced adhesive, and (b) adhesive containing PAN nanofibers.

Fig. 4. Typical load-displacement curves obtained from the DCB tests on PAN nanofiber-reinforced adhesives; (a) 1 g/m², (b) 2 g/m², (c) 3 g/m².

Fig. 5. R-curve for the non-reinforced and reinforced adhesives.

Fig. 6. SEM micrographs of (a) unreinforced adhesive and reinforced adhesive with (b) 1g/m², (c) 2g/m², (d) 3g/m² of PAN nanofibers.

Table 1. Specifications of adhesive UHU plus endfest 300 [25].

UHU endfest plus 300	
Chemical basis	Epoxy resin
Density	Binder: approx. 1.2 (g / cm ³) Hardener: approx. 0.96 (g / cm ³)
Viscosity	Binder: 40000 (mPa.sec) Hardener: 30000 (mPa.sec)
Pot life (20 °C)	90mins

Table 2. The mechanical properties of the adherends and adhesive.

Mechanical property	Adhesive (UHU® plus endfest 300)	Adherends (aluminum 7075-T651)
Elastic modulus (GPa)	2.0	70
Poisson's ratio	0.35	0.33
Tensile yield strength (MPa)	26.8	500
Tensile ultimate strength (MPa)	34.2	582
Elongation at break (%)	9.1	12.7

Table 3. Composition of etching solution for aluminum adherends [28].

Sulfuric acid (wt %)	27.5
Sodium dichromate (wt %)	7.5
Deionized water (wt %)	65

Table 4. Fracture energies obtained from experiments.

	Fracture energy, G_{IC} [N/mm]	Improvement*
Non-reinforced	0.11 ± 0.03	-
1 g/m ²	0.16 ± 0.05	45
2 g/m ²	0.25 ± 0.04	127
3 g/m ²	0.17 ± 0.09	55

* Improvement: $(G_{\text{reinforced}} - G_{\text{non-reinforced}}) / G_{\text{non-reinforced}} \times 100$.

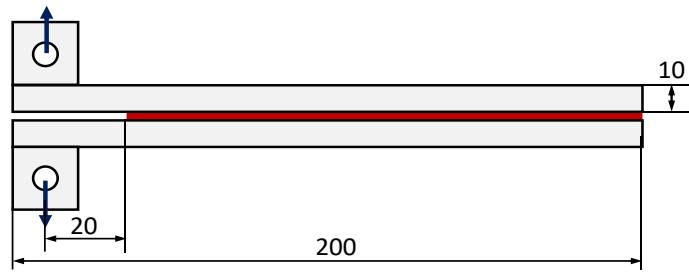


Fig. 1. Schematic geometry of the DCB test specimen (dimensions in mm).

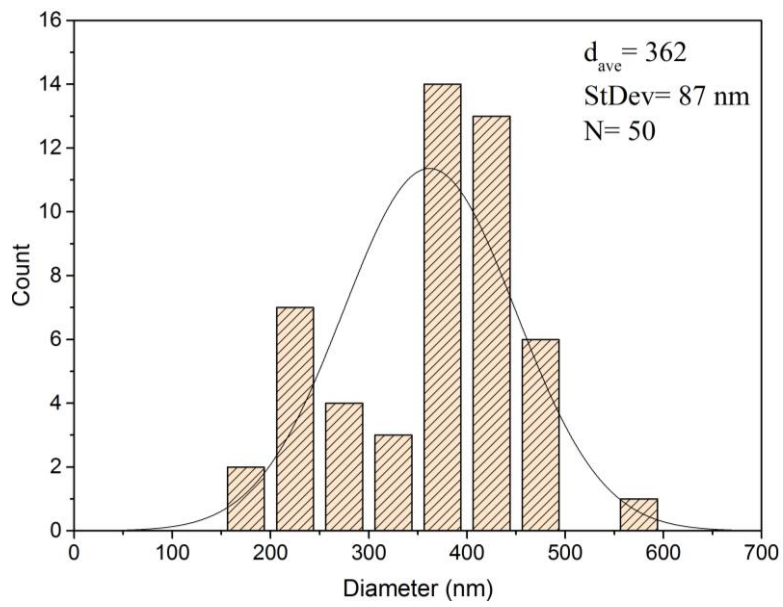


Fig. 2. Diameter distribution curve of PAN nanofibers.

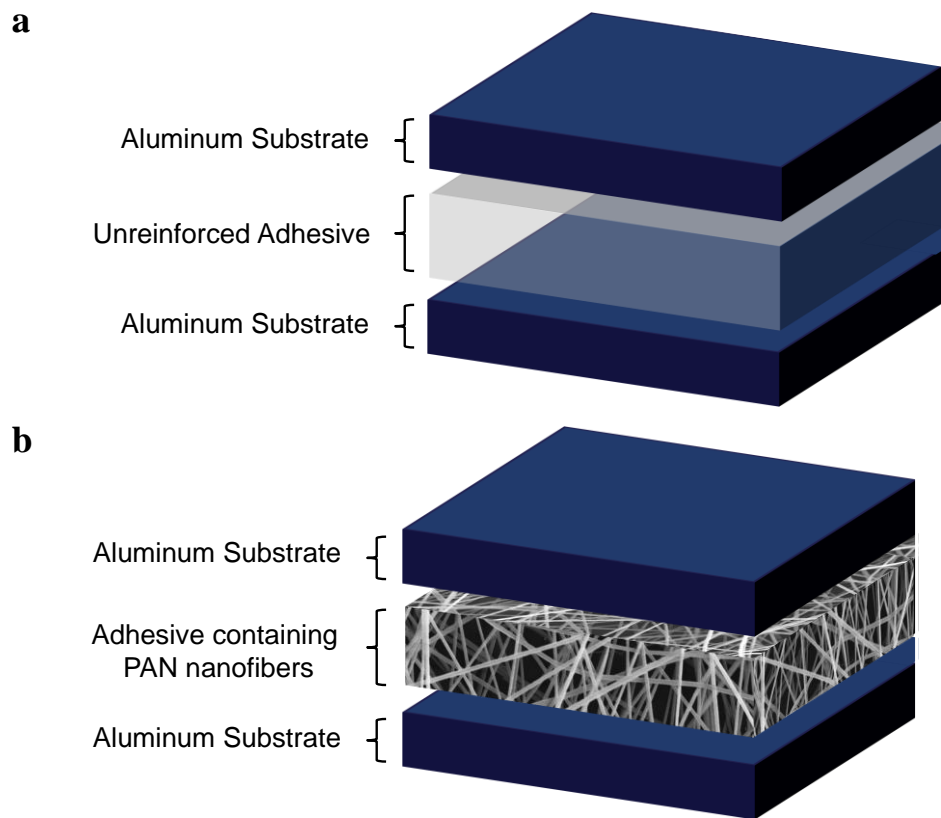
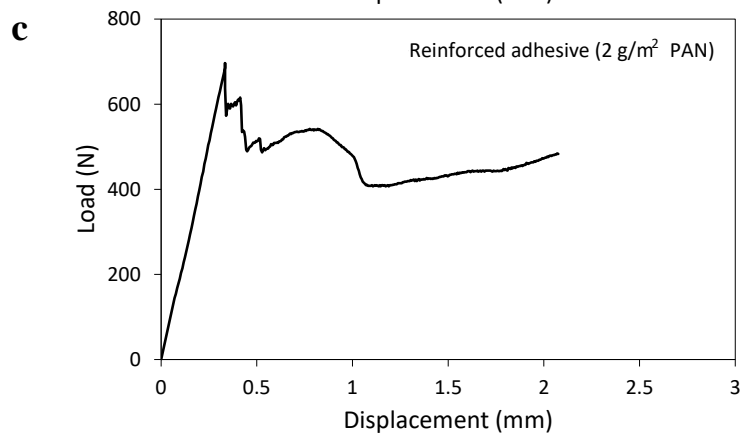
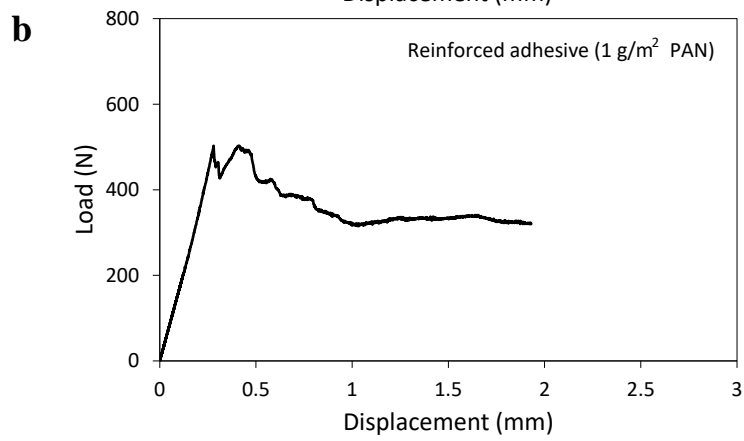
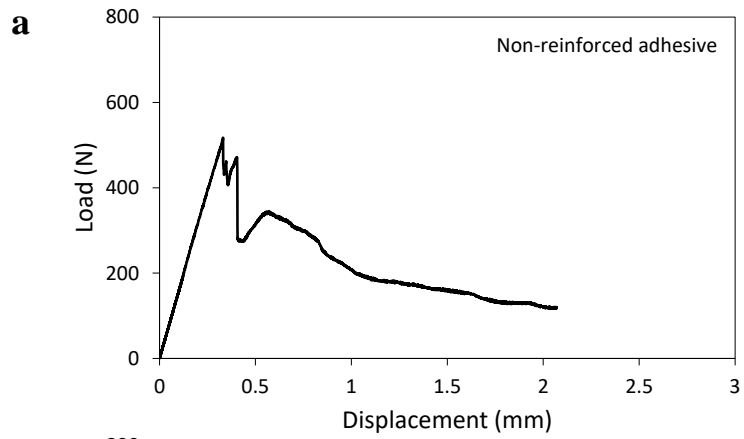


Fig. 3. Exploded view of adhesive joints bonded by (a) non-reinforced adhesive, and (b) adhesive containing PAN nanofibers.



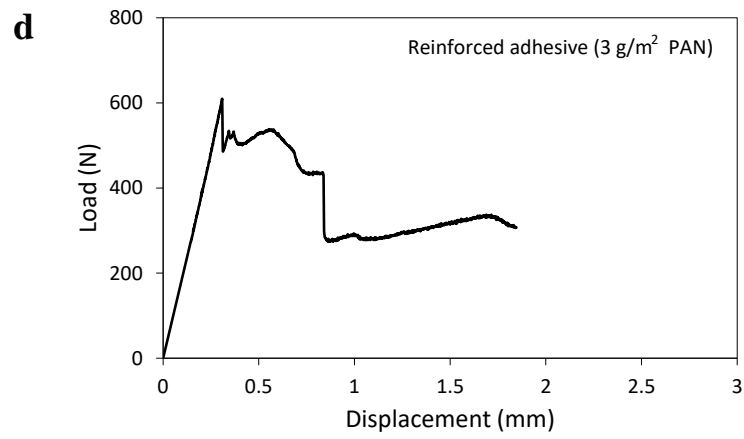


Fig. 4. Typical load-displacement curves obtained from the DCB tests on PAN nanofiber-reinforced adhesives; (a) 1 g/m², (b) 2 g/m², (c) 3 g/m².

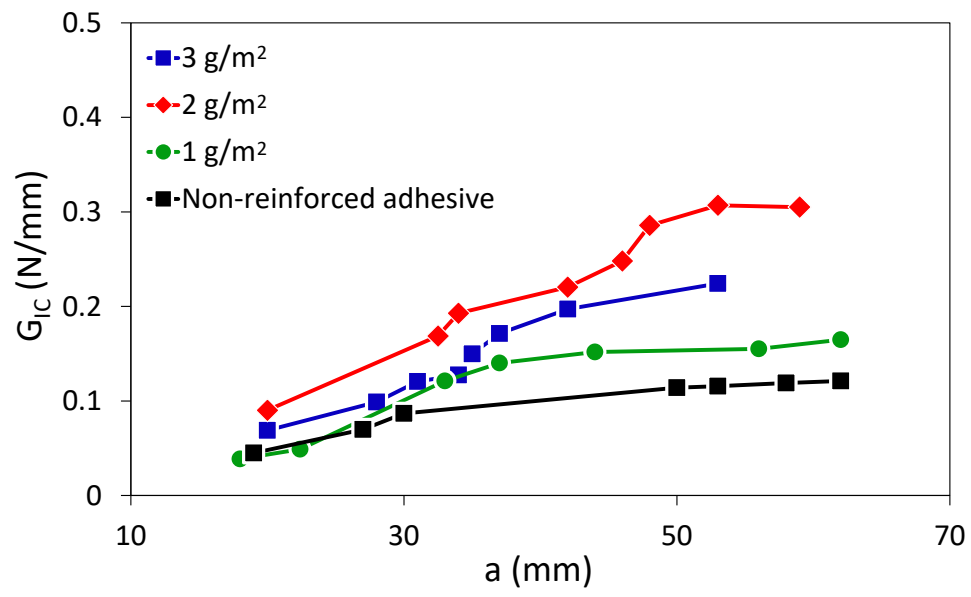


Fig. 5. R-curve for the non-reinforced and reinforced adhesives.

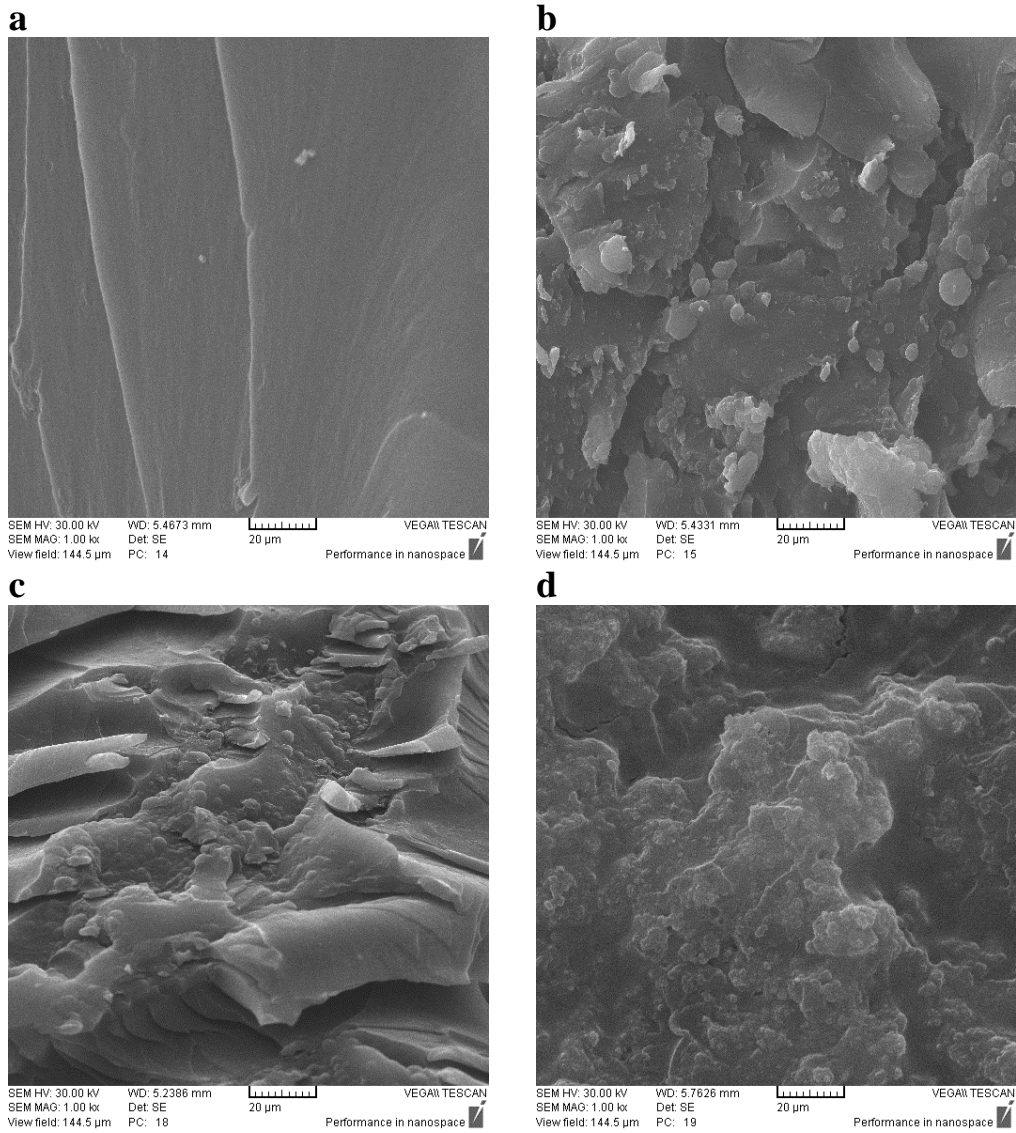


Fig. 6. SEM micrographs of (a) unreinforced adhesive and reinforced adhesive with (b) 1g/m^2 , (c) 2g/m^2 , (d) 3g/m^2 of PAN nanofibers.